Journal of Power Sources 207 (2012) 56–59

Contents lists available at SciVerse ScienceDirect

Journal of Power Sources

journal homepage: www.elsevier.com/locate/jpowsour

Short communication

Modelling of VRLA batteries over operational temperature range using Pseudo Random Binary Sequences☆

A.J. Fairweather[a,*], M.P. Foster[b], D.A. Stone[b]

[a] VxI Power Ltd, Station Road, North Hykeham, Lincoln LN63QY, UK
[b] Electrical Machines and Drives Research Group, Department of Electronic and Electrical Engineering, The University of Sheffield, Mappin Street, Sheffield S14DT, UK

ARTICLE INFO

Article history:
Received 17 October 2011
Received in revised form 19 January 2012
Accepted 6 February 2012
Available online 18 February 2012

Keywords:
Batteries
Modelling
State estimation
PRBS

ABSTRACT

This paper continues previous work concerning the use of maximum length sequences within parameter estimation for batteries. Using the familiar Randles' model batteries are examined over typical operational temperatures for variations in readily identifiable equivalent circuit parameters, using previously identified methods [1]. This analysis is used to present characteristics which can be subsequently used to inform the design of an online State-of-Charge (SoC) and State-of-Health (SoH) system for these batteries.

1. Introduction

Expanding applications for energy storage have led to a renewed focus on battery technologies and their optimisation. Much focus of this work involves the identification of the State-of-Function (SoF) of the batteries themselves. This performance indication is influenced by several factors, these being State-of-Charge (SoC), the age related State-of-Health (SoH), discharge rate, and the prevailing ambient temperature. Traditionally, specific gravity of the electrolyte was used as the primary indicator of battery state, and work continues in this area [2,3], however the rise in the use of Valve Regulated Lead Acid batteries precludes the use of these techniques generally. As such external means of performance evaluation, most notably coulomb counting [4], are used which generally require periodic recalibration to maintain accuracy.

It is well known that ambient temperature has a relationship to available capacity for lead acid batteries [5]. It therefore follows that any SoC measurement system must take into account this effect in order to report accurate results.

Previous work by the authors using the identification methods within this paper has led to the development of a system to identify state indicators within the battery [1,6] This paper extends this previous work using bandwidth limited white noise, in the form of Pseudo Random Binary Sequences (PRBS) to establish readily identifiable battery parameters. Correlations are sought between these parameters obtained in short duration tests to battery temperature in order to provide thermal calibration for a SoC/SoH evaluation system.

2. Modelling of batteries

Electrical representations of batteries allow analysis of the characteristics of the battery in terms which discard the complex electrochemical reactions during charge and discharge. Development of prognostic techniques for batteries in application relies on an adequate model to describe the processes involved. The work of Randles' [7] is widely regarded as the reference work in this field (Fig. 1).

R_i (Fig. 1) is the lumped resistance for the cell interconnections, etc. and represents the major series resistance for the cell. $C_{Surface}$ is a double layer capacitance, which is a result of the charge separation at the interface between the electrolyte and the cell plate [8]. R_t, in parallel with the double layer capacitance is the charge transfer resistance and is the electrical analogy of the inherent speed of the charge transfer reaction.

C_{Bulk} represents the dominant capacitive element of the cell, and the key performance indicators are the voltage developed across it (SoC) and the capacitance value itself which indicates State-of-Health.

The self-discharge resistance of the cell (R_d, shown as a load across the bulk element of capacitance) is typically high for a

☆ Presented at the LABAT'2011 Conference, Albena, Bulgaria, 7–10 June 2011.

* Corresponding author. Tel.: +44 1522500511; fax: +44 1522500515.
E-mail addresses: andrew.fairweather@vxipower.com (A.J. Fairweather), m.p.foster@sheffield.ac.uk (M.P. Foster), D.A.Stone@sheffield.ac.uk (D.A. Stone).

0378-7753/$ – see front matter © 2012 Elsevier B.V. All rights reserved.
doi:10.1016/j.jpowsour.2012.02.024

Nomenclature

a	PRBS amplitude
c	rated capacity (Ah)
C	capacitance (F)
C_{Bulk}	bulk capacitive element of cell (F)
$C_{Surface}$	double layer capacitance (F)
f	frequency (Hz)
I	current (A)
n	PRBS bits
N	PRBS sequence length
R_d	self discharge resistance (Ω)
R_i	series resistive element (Randle's circuit) (Ω)
R_t	charge transfer resistance (Ω)
t	PRBS clock period (s)
τ	time constant (s)
V	voltage (V)

healthy cell, and is most commonly quoted by the battery manufacturer in terms of a percentage discharge per month.

3. Battery testing and parameter estimation

Conventional methods of establishing parameters for the battery rely on controlled discharges, and application of pulse loads (Fig. 2). However, both of the methods are intrusive to the application, and the discharge test in particular requires a significant time period to run. Establishing R_d is particularly problematic, in that the battery under test must be left in an open circuit condition for a significant period of time (several weeks, dependant on the capacity of battery or cell) at constant temperature, with terminal voltage measurements taken periodically to determine self-discharge.

The tests are however useful in an analytical environment as a reference against which new battery testing methods can be verified. In this work the value of $C_{Surface}$ at 20 °C was established to verify the later results, along with a full set of parameters for the battery to establish a known state.

4. PRBS and frequency domain analysis

Maximum length sequences have been used in frequency response analysis over a range of applications for many years. In addition to parameter estimation [9], the sequences find applications spanning cryptography [10], audio frequency response [11] and control theory [12]. Suitable generators can be built using linear feedback shift registers [13], either in hardware or software. The digital sequence repeats periodically and the number of stages, n, defines the number of terms, N in the sequence.

$$N = (2^n - 1) \quad (1)$$

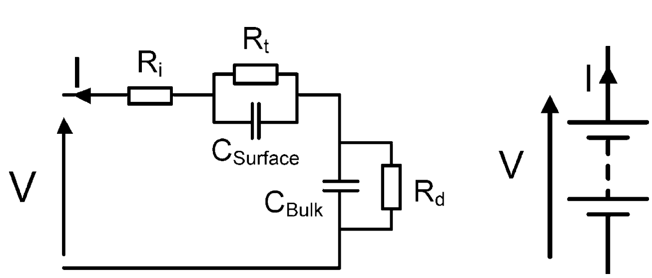

Fig. 1. Randles' model, with battery showing discharge current and terminal voltage.

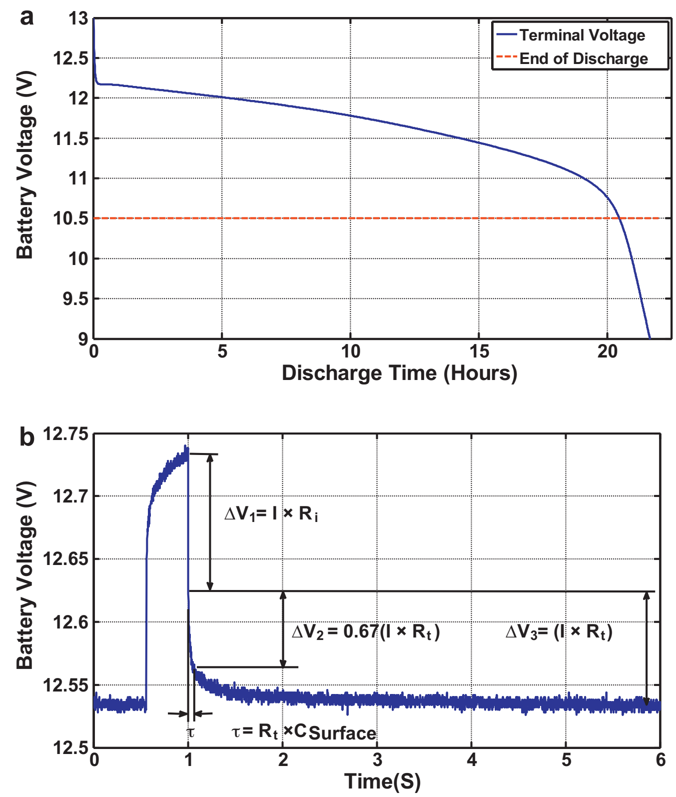

Fig. 2. (a) Typical discharge curve used to establish C_{Bulk} and (b) battery analysis using pulse loads.

The power spectrum of the maximum length PRBS will resemble that of white noise, and under Fourier analysis, the PRBS gives rise to a response which reaches zero at each multiple of the clock frequency (Fig. 3). The work of Davies [13] outlines the bandwidth limits of a PRBS by making reference to the clock period Δt.

$$f = \frac{1}{N\Delta t} \text{ to } f = \frac{1}{3\Delta t} \quad (2)$$

Using a PRBS with a suitable frequency spectrum will facilitate analysis of batteries in the frequency domain. The PRBS is used as a perturbation signal, being the control input of a constant current load module. Examination of terminal voltage deviations during this application of load, in conjunction with measurements of the current profile itself, allow off-line analysis using Fast Fourier Transformation (FFT). The obtained FFTs can the subsequently be used to obtain an impedance response for the battery under test.

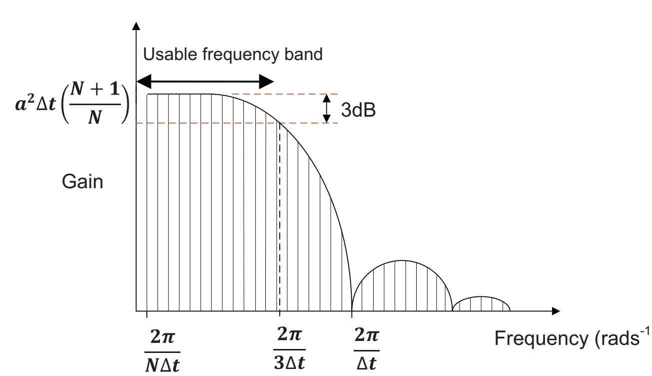

Fig. 3. Power spectrum (FFT) of a PRBS showing usable frequency band.

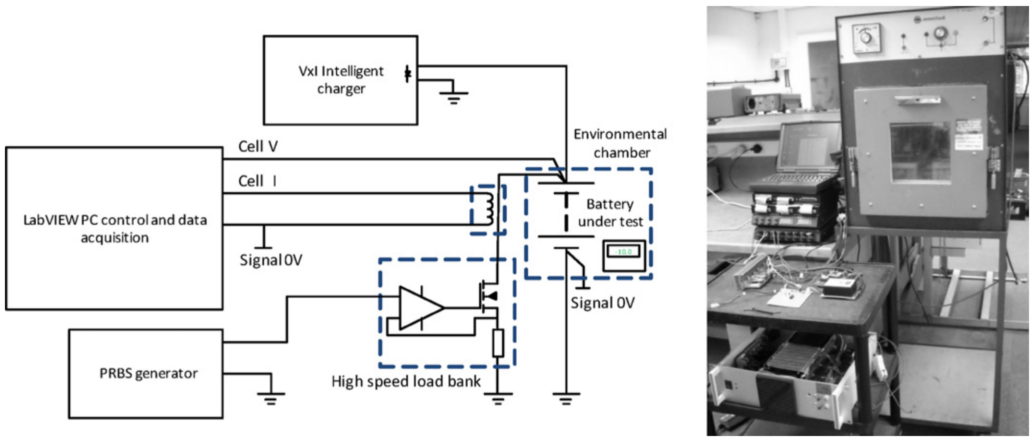

Fig. 4. Test system block diagram and photograph.

5. Correlations between SoC and $C_{Surface}$

Using $C_{Surface}$ as an indicator of SoC removes the requirement for long duration tests to establish C_{Bulk}. Previous work [14] in examining battery parameters using the PRBS technique identified correlations between $C_{Surface}$ and SoC, which suggested that the reducing activity within the battery or cell at low SoC is related to $C_{Surface}$.

This raised questions regarding the effect of temperature on battery performance, and, specifically the variation in $C_{Surface}$ with prevailing ambient operational conditions. The Arrhenius equation is well known and describes the change in the reaction rate with temperature of chemical processes generally. Within batteries, the effects of temperature and associated reaction speed manifest themselves as effects on service life and operational performance during discharge. Firstly at high temperature service life is reduced due to increased grid corrosion and other detrimental reactions. At the same time, discharge performance at high temperature is improved. Furthermore, it is known that at reduced ambient temperature lead-acid batteries experience a reduction in available capacity.

This therefore led to a hypothesis that changes in activity with a cell due to temperature could relate directly to $C_{Surface}$, and therefore suggested that characterising $C_{Surface}$ over operating temperature range would contribute as a suitable calibration factor for an evolving SoC/SoH measurement system.

6. Test system description

The system apparatus is shown in Fig. 4. The battery used was a 65 Ah VRLA battery manufactured by Yuasa (NPL65-12i) with a known history as a test sample. The test battery was situated within an environmental chamber at 100% SoC, remaining at each test temperature for several hours before the test. A battery backed power supply manufactured by VxI Power Ltd was used to provide charge between the tests, charge voltage being temperature compensated for the chamber conditions. The charge voltage compensation is carried out using a software map derived from manufacturer's data in conjunction with a temperature sensor on the battery itself. Nominal charge voltage is 2.28 V per cell at 20 °C, with this voltage being adjusted under digital control with changing battery temperature. During the test, the battery under examination is disconnected from the charger, and the PRBS perturbation applied. A high speed on board load is used for the PRBS sink current driven by a dSPIC^{TM} development board providing the signal input. The resulting current and voltage waveforms are captured using the integral data acquisition for subsequent off-line processing. A discharge test at the C/20 rate was then carried out to obtain a capacity

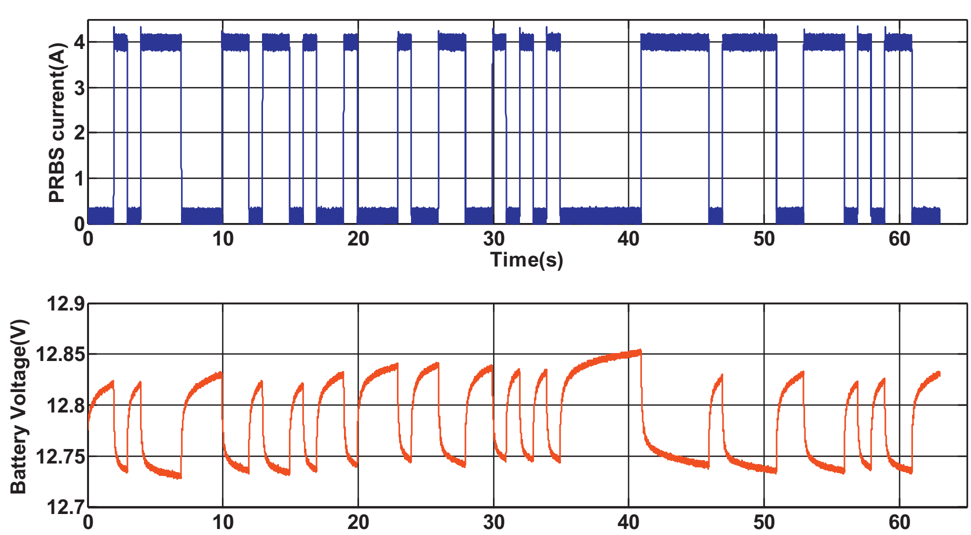

Fig. 5. Applied PRBS current and resultant battery terminal voltage during one of the tests.

Table 1
Measured battery capacity over test temperature range.

Temperature (°C)	−20	−10	0	10	20	30	40	50
Discharge time (h)	8.66	11.1	13.4	15.8	18.15	19.75	21.3	21.7
Capacity (Ah)	28.2	36.1	43.6	51.4	59.0	64.2	69.3	70.5

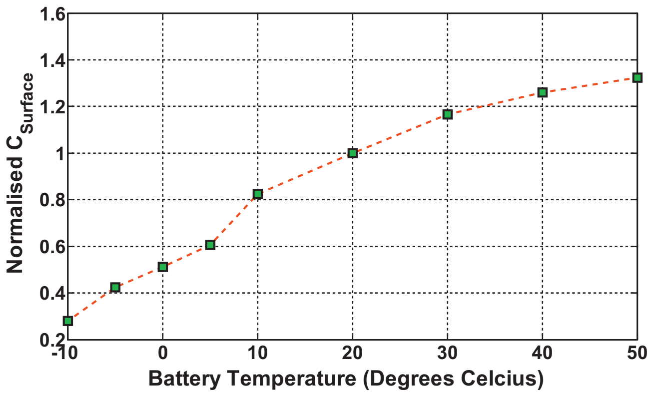

Fig. 6. Relationship between temperature and surface capacitance.

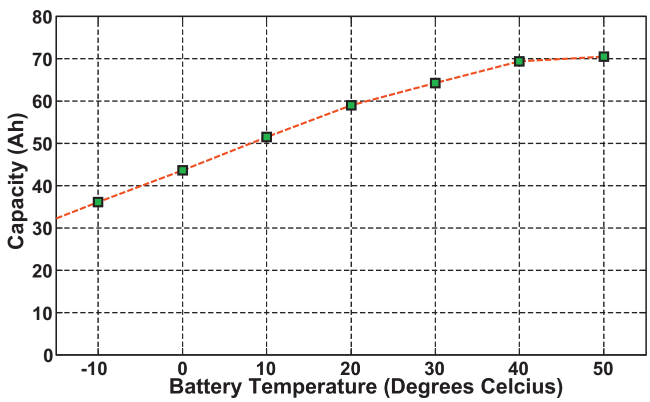

Fig. 7. Actual capacity of battery at test temperatures.

figure at this temperature. The process was then repeated for increments over the temperature range of the battery.

7. Test results

The batteries under test were examined over the temperature range of −10 °C to +50 °C, which represented typical operational temperature conditions for VRLA batteries in a standby application.

Fig. 5 shows the PRBS load pulses and a typical terminal voltage response obtained during one of the tests.

Using frequency domain analysis in Matlab, the PRBS test data provided information used to establish impedance responses. Further to this component values for Randles' circuit were examined, specifically $C_{Surface}$, using relationships established in previous work by the authors [6] shown in (3) below.

$$Z_{total} = \frac{1}{\sqrt{((1/R_d{}^2) + (1/XC_{Bulk}{}^2))}} + \frac{1}{\sqrt{((1/R_t{}^2) + (1/XC_{Surface}{}^2))}} + R_i + R_t \quad (3)$$

The relationship established between $C_{Surface}$ and battery temperature is shown in Fig. 6 with the data presented as normalised $C_{Surface}$ based on a temperature of 20 °C.

The observed trend in surface capacitance with reduced temperature was compared with actual battery capacity at the corresponding conditions. The discharge times obtained at the test temperatures gave rise to figures for Ah capacity at these points (Table 1) allowing a comparison to the PRBS test results. The obtained capacities are shown graphically in Fig. 7.

As temperature decreases the effective value of $C_{Surface}$ reduces, as the activity within the battery slows down. This follows the logic of the earlier findings of a variation in $C_{Surface}$ with available capacity. Considering the similarities of the responses in Figs. 6 and 7 indications point to the value of $C_{Surface}$ being one of the major processes controlling available capacity. These findings therefore suggest implementation of a thermally calibrated SoC system is possible using the battery testing methods outlined in this work.

8. Conclusion

Examination of the battery parameters using PRBS over the typical operating temperature range revealed a relationship with the value of $C_{Surface}$. Examination of battery capacity obtained during the tests at the various temperatures revealed general trends that could be correlated. These findings further validate the PRBS technique, as a method for establishing battery parameters, and that the technique is applicable over battery temperature range. The work gives rise to findings that further contribute to developing calibration algorithms for a PRBS based SoC/SoH system.

Opportunities for further work exist as a result of these findings, which include profiling a range of batteries, and examination of other battery chemistries.

References

[1] A.J. Fairweather, M.P. Foster, D.A. Stone, IET Conference Publications 2010 (CP563) (2010) TU244.
[2] J. Marcos-Acevedo, et al., Instrumentation and Measurement Technology Conference, 2009, I2MTC'09, IEEE, 2009.
[3] Y. Guo, Sensors and Actuators B: Chemical 105 (2) (2005) 194–198.
[4] K.S. Ng, et al., Applied Energy 86 (9) (2009) 1506–1511.
[5] Yuasa NP Valve Regulated Lead Acid Battery Manual, Yuasa Battery Corporation, 1999.
[6] A.J. Fairweather, M.P. Foster, D.A. Stone, EVS 25, Shenzhen, China, 2010, EVS25–K5LPPH08.
[7] J.E. Randles, Discussions of the Faraday Society (1) (1947) 11.
[8] D. Linden, Handbook of Batteries, 2nd ed., McGraw-Hill, New York, 1995, 1 v. (various pagings).
[9] H.J. Vermeulen, J.M. Strauss, V. Shikoana, Power Engineering Society General Meeting, 2003, IEEE, 2003.
[10] T.M.M. Cedric, R.W. Adi, I. McLoughlin, TENCON 2000, Proceedings, 2000, pp. 275–278.
[11] D.G. Jamieson, T. Schneider, Engineering in Medicine and Biology Magazine, IEEE 13 (2) (1994) 249–254.
[12] B. Miao, R. Zane, D. Maksimovic, IEEE Transactions on Power Electronics 20 (5) (2005) 1093–1099.
[13] W.D.T. Davies, System Identification for Self-Adaptive Control, Wiley-Interscience, London/New York, 1970, xiv + 380 pp.
[14] A.J. Fairweather, M.P. Foster, D.A. Stone, PCIM Europe 2011, Nuremberg, Germany, 2011, pp. 515–520.